

Theoretical Evidence for Temperature-induced Proton Mobility in Isolated Lysine-rich Polyalanines

F. Calvo* and Ph. Dugourd

Laboratoire de Spectrométrie Ionique et Moléculaire (LASIM), Université Claude Bernard Lyon 1, 43 Bd du 11 Novembre 1918, F69622 Villeurbanne Cedex, France

Received: December 14, 2007

A multistate molecular mechanics method is introduced to model the possible competition between various protonation sites in gas-phase biomolecules with excess protons. The method relies on the Amber force field for each site and is calibrated against density-functional theory benchmark calculations at the 6-31+G(d,p) level. In its adiabatic version, where it has similarities with constant-pH algorithms, the model predicts that the small protonated Ala₄-Lys peptide, unprotected at the N-terminus, changes protonation site above 400 K. In the larger [Ala₉-Lys+H]⁺ peptide, the proton remains at the lysine amine group in a favored charge/electric dipole conformation. In the three-state Ala₄-Lys-Ala₄-Lys peptide, the excess proton is found to be partially delocalized on the amine group of the first lysine and on the N-terminus. The statistical properties of the protonated peptides are found to significantly depend on the localized character of the proton. Finally, the model is extended by considering possible couplings between the protonation sites, in an empirical valence-bond version. Strong couplings can stabilize the peptides into unexpected proton-bound conformations over broad ranges of temperature.

Introduction

Proton transfer across hydrogen bonds plays an important role in determining the biological functions of many molecules.¹ In the condensed phase, enzymatic activity² is catalyzed by proton transport, and the diffusion through ion channels is enhanced by reversible protonation/deprotonation of basic residues.³ In the gas phase, the migration of protons in ionized peptides has been invoked to interpret the heterogeneous fragmentation patterns observed in various mass spectrometry experiments.^{4–15} Understanding how these patterns emerge from the molecular details would greatly improve our ability of microsequencing peptides, which in turn would be beneficial in proteomics.¹⁶ Low-energy collision-induced dissociation experiments^{8,17–19} indicate that intramolecular proton transfer takes place subsequent to collisional activation, mainly leading to charge-driven fragmentation by cleavage at the amide bonds (into the so-called b and y ions). At high energies, the ions produced by collisions likely depend on the location of the basic residues along the backbone.⁴ Ion mobility²⁰ and infrared spectroscopy measurements²¹ have since further supported this mobile proton model.

Hydrogen/deuterium exchange studies have provided additional evidence for intramolecular proton transfer in peptides.^{22–24} In particular, it was suggested that hydrogen atoms attached to nitrogen and oxygen can be completely randomized prior to dissociation, a process also referred to as “scrambling.”²⁵ However, contrasting measurements have recently questioned the extent of scrambling in gas-phase peptides.^{26–28}

On the theoretical side, several groups have performed extensive first-principle calculations of the potential energy surface (PES) of protonated peptides.^{14,29–34} These studies generally aim at calculating gas-phase basicities or proton affinities,^{29,31–35} mapping the stationary points to identify the structure of fragments^{14,32} or to estimate intramolecular reaction rate constants through transition state theories.³⁰ Even using

powerful methods such as density-functional theory (DFT) with hybrid functionals and large basis sets, such calculations are computationally costly and are currently limited to a few small amino acids. Polyglycines, in particular, have received special attention,^{14,32,36} largely due to existing experimental data.^{37,38}

The preferred protonation sites in a gas-phase peptide are mostly determined by the relative basicities and proton affinities.³⁹ Unfortunately, these quantities are hard to measure experimentally, due to the difficulty of accessing gas-phase data in general. In particular, and despite recent progresses in bracketing techniques,³⁵ disagreements between several methods have been reported in the important case of peptides with basic residues.⁴⁰ The influence of protonation site on the relative stability of molecular conformation has been theoretically illustrated by Maksic and Kovacevic.⁴¹ These authors found that the side chains of lysine and glutamine are preferentially protonated at the expense of the alpha amine, by forming an extra hydrogen bond with the dangling carbonyl group of the backbone. These findings are consistent with ion mobility measurements from the Jarrold group.^{38,42} More generally, it is well-known that the proton affinity depends on molecular conformation.^{29,31,33,36,43} This may have significant consequences for large peptides, which can undergo some important heating upon collision and acquire some flexibility. In particular, peptides having several basic residues may swap protonation site depending on temperature, as a result of conformational changes such as unfolding. Such behavior has recently been inferred from ion mobility measurements on polyalanines with arginine and lysine residues at both ends.⁴⁴ In this paper, we report similar evidence from theoretical modeling.

While first-principle electronic structure methods can currently locate the most stable conformation of small protonated polypeptides, they do not account for the floppyness arising from the rather high temperature in beams or traps. Accounting for temperature effects at first-principle levels can be partially achieved by performing Car-Parrinello (CP) molecular dynam-

* Corresponding author e-mail: fcalvo@lasim.univ-lyon1.fr.

ics trajectories. However, sampling the rugged energy landscape of peptides in an ergodic way remains a difficult issue, which is not tractable even with the help of the CP method. Investigating a broad range of conformations at a finite temperature is thus beyond the reach of present electronic structure approaches, and simplifications are necessary.

The standard method for sampling molecular conformations is molecular mechanics, through popular force fields such as CHARMM,⁴⁵ Amber,⁴⁶ or Gromos.⁴⁷ However, such methods do not account for bond breaking, hence they are not appropriate for explicitly describing proton transfer. Dissociative potentials based on the Stillinger–David model for water,⁴⁸ especially its more recent extensions,^{49,50} are fully flexible, making them numerically expensive and suitable for molecular dynamics⁵¹ rather than large-amplitude conformational sampling. Moreover, as criticized by Haymet and Oxtoby,⁵² their chemical foundations are unclear. Two classes of alternative approaches can be considered. Constant-pH methods^{53–58} have mainly been designed for hydrated molecules and a variable number of protonation sites (grand canonical ensemble). Usually, each change in the protonation state is accompanied with a short molecular dynamics (MD) simulation, followed by an acceptance or a rejection by a Monte Carlo procedure.^{56,58} The empirical valence-bond (EVB) approach, originally developed by Warshel for molecular simulation² and developed independently for protonated water by Vuilleumier and Borgis⁵⁹ and by Schmitt and Voth,⁶⁰ is an explicit reactive description, in which the proton is quantum mechanically delocalized over several sites forming as many elements of a basis set. The EVB model has been applied to the dissociation of weak acids⁶¹ and to the dynamics of biological ion channels.⁶² In closer relation to the present work, it has been extended to histidine and glutamic acid in contact with water clusters.⁶³ The EVB approach to proton solvation in aqueous and biomolecular systems has recently been reviewed by Swanson and co-workers.⁶⁴

We borrow several ideas from the aforementioned methods as an attempt to model polypeptides with multiple protonation states, in a common framework suitable for sampling flexible conformations at finite temperatures. Our method is essentially an EVB-type model relying on the Amber force field for each fixed protonation site. We mainly consider an adiabatic model, where in absence of any coupling the proton occupies at each conformation the most energetically favorable site. This adiabatic approximation is formally equivalent to the constant-pH algorithms developed by several authors.^{56,58} We also illustrate the possible effects of an attractive coupling between the protonation sites. The peptides considered in the present work are unprotected, contain between four and nine alanines along with one or two lysine residues and a single excess proton. Thus, they have two or three basic amine protonation sites, at the alpha N-terminus and at the end of the lysine side chains. Because of the discrepancies between the various experimental and theoretical sources, the relative basicities of these groups have not been imported from the literature; instead, they have been recalibrated using dedicated DFT calculations. Our results, which strongly support the mobile proton model, indicate that the equilibrium properties of such protonated peptides can qualitatively disagree with calculations assuming that the proton is rigidly fixed to the most basic sites.

The main details of our model are given in the next section, and the results for the peptides A₄K, A₉K, and A₄KA₄K (A = alanine, K = lysine) with one excess proton are discussed in the subsequent section.

Methods

The conformations of the peptides considered in this work are described by sets of internal coordinates (dihedral angles of the backbone and side chains), keeping the bond lengths and bond angles fixed. We limit the present discussion to molecules having several amine groups, where the protonation state only moderately influences the geometry of its neighborhood. For each conformation, the molecule can exist in a finite number of protonation states Γ , and we denote by \mathbf{R}_α the conformation where the proton is carried by state $\alpha \in \Gamma$. A given conformation \mathbf{R} can support several states α with the same set of coordinates, only differing in the location of the excess proton to a particular amine group.

Adiabatic Model. The potential energy E_α of the molecule with conformation \mathbf{R}_α within state α is modeled by a molecular mechanics force field, whose parameters only depend on the protonation state. The dependence on the latter is taken through a parameter b_α , which by definition does not depend on conformation (eq 1).

$$E_\alpha(\mathbf{R}_\alpha) = E_{\text{FF}}(\mathbf{R}, \alpha) + b_\alpha \quad (1)$$

The additional energies $\{b_\alpha, \alpha \in \Gamma\}$ play the role of instantaneous proton affinities, and measure the cost of forming covalent bonds between the proton and the various states α . In the case of a two-state model HA and A⁻, the relative values of b_α are directly related to the pK_a through the calculation of a free-energy difference between the two force fields E_{HA} and E_{A^-} .⁵⁸ For a given conformation \mathbf{R} , the energies E_α of the various protonation states differ due to conformation and to the state itself, notably through the b_α parameters.

In constant-pH algorithms, the pK_a parameters are fixed in advance, and the pH influences the probabilities to find the system as HA or A⁻. The parameters b_α must then be optimized in order that these probabilities reach the required value of the pH.^{56,58} In such approaches, the number of protons is not a conserved quantity, as it depends on the pH. In the present work, we deal with gas-phase molecules that can only exchange protons by intramolecular transfer. For a given conformation \mathbf{R} and its various states $\{\alpha\}$, the most likely protonation state is the one with lowest energy $E_\alpha(\mathbf{R}_\alpha)$. We thus define the global potential energy of conformation \mathbf{R} in an adiabatic model as eq 2.

$$E_{\text{adiab}}(\mathbf{R}) = \min_{\alpha} \{E_\alpha(\mathbf{R}_\alpha)\} \quad (2)$$

By analogy with quantum mechanics, the state α that minimizes the adiabatic energy will be referred to as the ground state.

The main ingredients of this model are a reliable force field consistent for the various protonation states, as well as an estimation of the constants b_α . Following our previous investigations,⁶⁵ we have chosen the Amber force field⁴⁶ with its ff96 parameters set,⁶⁶ as they correctly reproduce experimental measurements on small protonated gas-phase molecules. The partial charges of Amber ff96, which were originally increased with respect to their gas-phase values in order to compensate for polarization effects in solution, have been partially shielded here by using a dielectric constant $\epsilon_r = 2$.

Calibration by DFT. The peptides considered in this work are not hydrated, hence there is no reservoir of protons that could impose a pH. In addition, they are highly flexible at high temperatures, making the proton affinities known in single amino-acids and small peptides³⁹ poorly relevant here.⁴¹

Quantum chemical calculations have been undertaken to determine the constants b_α corresponding to the various proto-

TABLE 1: Potential Energies of Extended Conformations of Small Protonated Peptides, Obtained with Amber ff96 and by DFT Calculations with the B3LYP Functional and the 6-31+G(d,p) Basis Set

molecule and protonation state	Amber ff96 energy (kcal/mol)	B3LYP 6-31+G(d,p) energy (kcal/mol)
H ⁺ A ₄ K	16.12	0
A ₄ [KH ⁺]	61.10	3.84
H ⁺ A ₉ K	55.56	0
A ₉ [KH ⁺]	101.36	6.60
H ⁺ [A ₄ K*A ₄ K]	154.01	0
A ₄ [K*H ⁺]A ₄ K	194.67	-2.61
A ₄ K*A ₄ [KH ⁺]	199.86	6.75

nation states on the amine groups of the following peptides: A₄K, A₉K, and A₄KA₄K. The latter peptide will be denoted as A₄K*A₄K, as a way to distinguish the two basic lysine groups K* and K along the peptide sequence. Density-functional theory was chosen for its ability to handle such rather large molecules, and following the recommendations of Dinadayalane and co-workers,⁶⁷ we have chosen the hybrid functional B3LYP with a Pople-type basis set,⁶⁸ taken here as 6-31+G(d,p). To minimize the contribution of dispersion energy, which is not correctly accounted for by DFT, we have calibrated the b_α constants on fully extended conformations of the peptides with ϕ and ψ angles both equal to 180°. These geometries have not been optimized; hence, the proton affinities found are not necessarily equal to the values measured or calculated for stable conformations at higher levels. From the absolute energies and the Amber energies, the constants b_α are straightforwardly obtained for these extended conformations.

The values of the absolute Amber ff96 energies, DFT energies, and constants b are given in Table 1 for the three peptides considered here and for their various protonation sites.

Because of the arbitrary reference of potential energies, only the differences between the constants b_α and a specific value are relevant. For the DFT calculations, we have thus considered the protonation site on the α NH₂ group as the reference. As can be seen from Table 1, this state is the more stable of the A_nK peptides in extended conformations, in agreement with the first-principles study by Karsic and Kovacevic.⁴¹ This unusual protonation at the N-terminal amino group suggests that this should be the most stable state at very high temperatures, where the extended conformations are most likely. However, as will be shown below, low temperatures favor more compact conformations, and it can be very advantageous to locate the proton on the lysine end, consistently with the expected behavior. In the case of A₄K*A₄K, the two lysine residues are clearly not equivalent, and the first lysine turns out to be the most favorable protonation state in this reference conformation.

The energies given in the table cannot be used to draw any conclusion yet about the preferred protonation sites in real peptides, because their extended conformation was taken as an arbitrary but convenient choice. Sampling at a finite temperature will precisely allow us to estimate the relative occupancies of the various sites.

Couplings: Empirical Valence-Bond Model. The atomistic mechanisms of proton transfer in aqueous media involve bond breaking and bond formation. In condensed water, resonance phenomena on the delocalized proton can stabilize water-hydronium complexes such as the Zundel H₅O₂⁺ or Eigen H₉O₄⁺ cations. The chemistry of proton transport in water and in aqueous biomolecules is qualitatively and quantitatively

described by multistate empirical valence-bond models,^{59,60,63} and we use a similar strategy here as a natural extension of the adiabatic model presented in the previous section.

Each conformation **R** is still described as a set of various protonation states $\alpha \in \Gamma$, each having its potential energy defined by eq 2 with the constant b_α as determined by DFT benchmark calculations. The state α is now considered as a diabatic member $|\alpha\rangle$ of a basis set. The excess proton is delocalized over all valence bond states by introducing a wave function Ψ expanded on the basis set as eq 3,⁶⁹

$$\Psi = \sum_{\alpha} c_{\alpha} |\alpha\rangle \quad (3)$$

where $\{c_{\alpha}\}$ are a set of unknown coefficients. The ground-state of the system is obtained by matrix diagonalization of the Hamiltonian **H**,

$$\mathbf{H}\mathbf{c} = \mathbf{S}\mathbf{c}\mathbf{E} \quad (4)$$

where **S** is the overlap matrix. We assume in the following that the valence-bond states form an orthonormal basis, that is $S_{\alpha\alpha'} = \delta_{\alpha\alpha'}$. The diagonal elements $H_{\alpha\alpha}$ of the EVB Hamiltonian are given by the energies E_{α} , and the couplings $H_{\alpha\alpha'}$ are determined by the nondiagonal elements shown in eq 5.

$$H_{\alpha\alpha} = \langle \alpha | \mathbf{H} | \alpha \rangle = E_{\alpha}, \quad H_{\alpha\alpha'} = \langle \alpha' | \mathbf{H} | \alpha \rangle = \langle \alpha | \mathbf{H} | \alpha' \rangle \quad (5)$$

The coupling $H_{\alpha\alpha'}$ between states α and α' acts to stabilize particular conformations, as a way to model charge resonance in complexes with delocalized protons. In their EVB model for protonated water, Schmitt and Voth⁶⁰ have used a many-body expression for the coupling as a function of conformation, by comparing the current geometry to that of the Zundel cation. Here we follow the simpler approach of Vuilleumier and Borgis,⁵⁹ who modeled the off-diagonal coupling terms only based on the atoms involved in the proton exchange. In our model, the coupling between states α and α' depends on the distance $d_{\alpha\alpha'}$ between the amine nitrogens of each state. A chemically intuitive requirement for this coupling is that it decays as the distance increases. In this purpose we introduce a typical interaction length d_0 , the range ρ for the coupling and a magnitude D . A simple Fermi-like expression for $H_{\alpha\alpha'}$ was chosen here because it naturally meets the requirements of a monotonically decreasing function over a finite distance interval;

$$H_{\alpha\alpha'} = \frac{D}{1 + \exp[\rho(d_{\alpha\alpha'} - d_0)]} \quad (6)$$

D will be taken as positive (attractive coupling), but the case of negative values leading to repulsive coupling, though less realistic, could be studied as well. At each conformation, the EVB matrix **H** is diagonalized into the set of coefficients $\{c_{\alpha}\}$ and energy levels \tilde{E}_{α} . The ground state Ψ_0 is now a linear combination of fixed proton states with weights $c_{\alpha}^{(0)}$ and with a resulting energy E_{GS} . The proton is partially delocalized over each state α with a corresponding weight $w_{\alpha} = [c_{\alpha}^{(0)}]^2$.

In the absence of coupling ($D = 0$), the Hamiltonian matrix is diagonal, and the ground-state is the lowest diagonal element, with weight 1. The adiabatic model considered in the previous section is thus a special case of the more general EVB approach.

Simulation Protocol. The potential energy surfaces of the above models for delocalized protons have been sampled using Monte Carlo simulations in the canonical ensemble. The MC moves were performed in the space of dihedral angles, rotating bonds accordingly by drawing a random angle $\delta\theta$ in the range $-\theta_{\max} \leq \delta\theta \leq \theta_{\max}$, with θ_{\max} an amplitude adjusted in order to get about 50% acceptance rate. Torsion angles are also

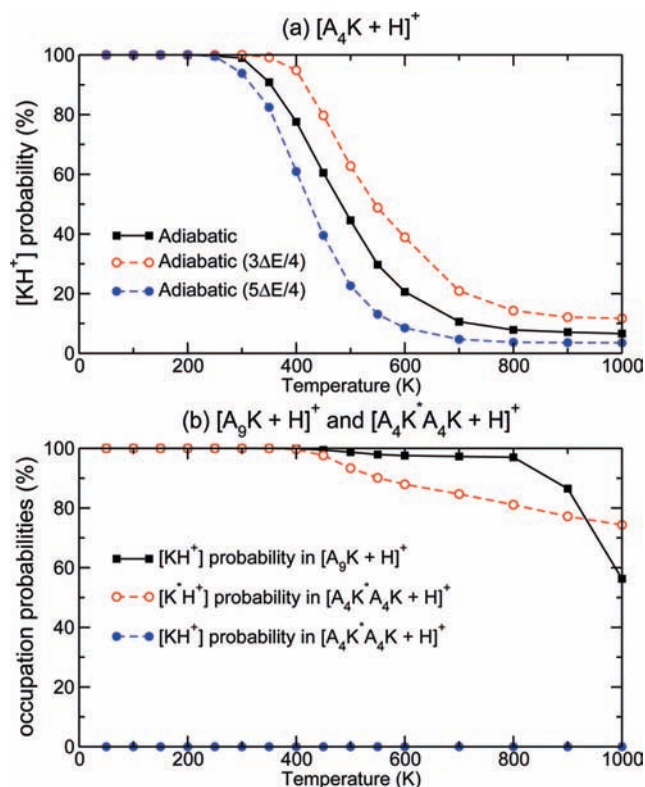


Figure 1. Occupation probability of the excess proton on various sites of the A_4K , A_9K , and $A_4K^*A_4K$ peptides, in the adiabatic model. (a) Probability of finding the proton on the amine end of the lysine in A_4K , obtained with energy gap ΔE taken as the DFT/B3LYP/6-31+G(d,p) value or varied by $\pm 25\%$. (b) Probability of finding the proton on the amine end of the lysine in A_9K , and on the amine end of each lysine K and K^* .

randomly drawn with equal probability. At each conformation, the energy obtained from the Hamiltonian matrix, E_{GS} , or its adiabatic value E_{adiab} , whose evaluation does not require diagonalization, is compared to the same energy at the previous conformation and is accepted according to a Metropolis criterion. The simulations have been performed in the temperature range 50–1000 K, starting at 1000 K and reducing the temperature in steps of 100 K down to 600 K, and subsequently in steps of 50 K down to 50 K. Each of these MC trajectories consisted of 5×10^6 Monte Carlo cycles, following 10^6 cycles left out for equilibration. The first trajectories at 1000 K were initiated in the fully extended conformation used to calibrate the constants b_α by DFT. From these MC simulations, the thermodynamical properties at equilibrium have been obtained by processing the distributions of potential energy using the multiple histogram method.⁷⁰

To investigate the effects of the delocalized proton, Monte Carlo simulations have also been carried out for each peptide with the excess proton fixed on each of the amine groups. These latter simulations have been improved with the all-exchange parallel tempering strategy^{71,72} to accelerate convergence.

Results

Delocalization in the Adiabatic Model. The average occupation probabilities of the proton on the various states of the A_4K , A_9K , and $A_4K^*A_4K$ peptides, as obtained from the adiabatic model, are shown in Figure 1. A_4K has been considered as a test case. For such a two-state model, the relative occupancy of the proton depends on the energy difference $\Delta E = b_1 - b_0$ between the two states $1 = A_4[KH^+]$ and $0 =$

H^+A_4K . The possible inaccuracies of the force field and DFT calculations have been addressed by repeating the simulations for ΔE taken as 75 or 125% of its value computed at the B3LYP/6-31+G(d,p) level.

As seen in Figure 1a, the protonation state is more likely to be at the N-terminal end at high temperature, but changes and localizes at the lysine end below about 400 K. The preferred state found at high temperature is consistent with the extended nature of the peptide, where hydrogen bonds are broken.⁴¹ At low temperature, conformational changes associated with the folding transition are evidenced on the proton transfer to the lysine end. Increasing (decreasing) the energy gap ΔE does not modify the curves qualitatively beyond a shift of ≈ 50 K to lower (higher) temperatures. This shift was expected, because it readily determines the stability of the protonated lysine relative to the protonated alpha amine. The rather small effect of changing ΔE shows the robustness of our adiabatic model and confirms experimental suggestions by Kohtani et al.⁴⁴ that proton transfer can be triggered by conformational changes.

In the larger peptide A_9K , the proton is mainly stable on the C-terminus lysine amine end group—up to high temperatures. Only above 800 K does the proton become partially localized on the alpha- NH_2 end site, in agreement with the positive gap ΔE , which provides an estimate of the energy loss when protonating the lysine in extended conformation. The protonation on the C-terminus lysine indicates that the molecular conformation is not fully extended, possibly suggesting some residual hydrogen bonds in the intermediate range 500–800 K.

The $[A_4K^*A_4K + H]^+$ peptide has three possible protonation sites. As seen from Figure 1 the proton has a clear tendency of occupy the end group of the K^* residue. Above 500 K, the end group of the other lysine K remains essentially unprotonated, meaning that the proton is partially delocalized on the alpha amine.

Influence of Proton Delocalization on Equilibrium Properties. The variations of the heat capacities of the protonated A_4K peptide obtained assuming fixed locations of the proton, or a delocalized proton within the adiabatic model, are represented in Figure 2.

The heat capacities of the two peptides with fixed protonation state both exhibit two peaks, indicative of the unfolding transition preceded by finite-size, “premelting” effects likely associated with structural phase changes. The locations and the widths of these peaks are, however, very different for the two states. Because the proton is localized on the lysine, the unfolding transition is very broad over the temperature range 200–800 K. If the alpha amine carries the proton, then unfolding takes place at much lower temperatures and is also a sharper process. Protonation of the lysine is, thus, energetically and thermally more stable. The protonation state greatly influences the thermal behavior of the peptide, and the resulting heat capacity shows greater similarity with the protonated lysine at low temperature and with the protonated alpha amine at high temperature, as expected from the corresponding weights seen in Figure 1a.

The more stable conformations found for the two models, represented in Figure 2, reveal qualitative differences that explain this behavior. In both protonation states, the lowest energy conformation is essentially globular. In the protonated lysine case, the two amine groups are on opposite sides of a plane formed by the backbone, and three carbonyl groups are oriented toward the NH_3^+ group in very favorable hydrogen-

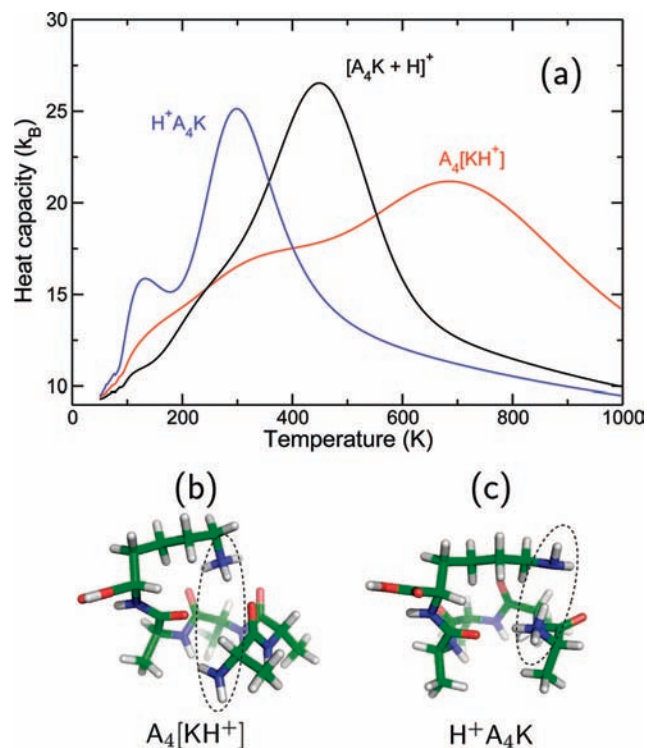


Figure 2. (a) Heat capacity of the $[A_4K + H]^+$ peptide obtained for the delocalized proton with the adiabatic model (black line), or assuming that the proton is fixed at the lysine amine group (red line) or at the terminus amine group (blue line). The most stable conformations of the two latter peptides are shown in panels (b) and (c), respectively, the proximity of the two amine groups is highlighted by dashed ellipses.

bond-like interactions. If the proton lies at the alpha amine end, no particular hydrogen bond is formed involving the protonated amine.

The heat capacities of protonated A_9K , shown in Figure 3, suggest a sharper unfolding transition near 420 K, albeit a significant shoulder is found on the high-temperature side. If the proton is kept fixed on the alpha amine, the transition temperature is higher (600 K) and a low-temperature premelting shoulder occurs at 250 K. Assuming that the proton is localized on the lysine accounts for the general variations of the heat capacity, in agreement with its strong localization on this site reported in Figure 1b. The most stable structure found for the peptide greatly differs depending on the proton location. The protonated C-terminus lysine forms capping hydrogen bonds with the helical backbone and interacts very favorably with the electric dipole of this short α helix, as seen in Figure 3b. Both effects are well-known in the literature.^{73,74} Conversely, the lowest-energy conformation of the A_9K peptide protonated at its N-terminus is globular, as seen in Figure 3c.

In agreement with ion mobility measurements³⁸ and with recent molecular simulations,⁷⁵ we interpret the higher stability of the protonated lysine state of the A_9K peptide as due to the favorable interaction with the helix. Above 450 K the peptide unfolds, but the protonated lysine is still able to form partial helices³⁸ as well as H-bonds with the oxygen of the closest backbone carbonyl, thus delaying proton transfer until the temperature exceeds 800 K.

The third peptide considered in this work, $A_4K^*A_4K$, has three possible protonation sites, and the corresponding heat capacities obtained for each of these fixed sites are reported in Figure 4 along with the curve for the delocalized proton in the adiabatic model.

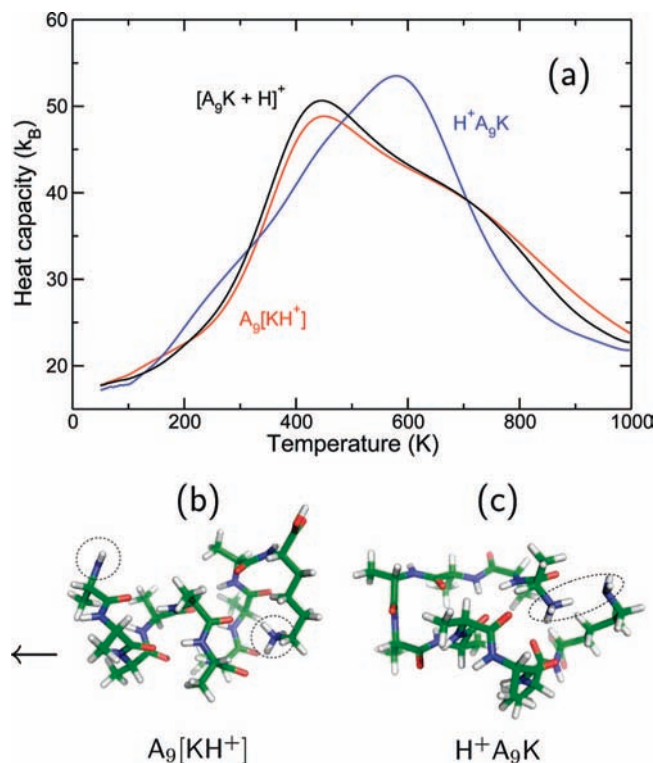


Figure 3. (a) Heat capacity of the $[A_9K + H]^+$ peptide obtained for the delocalized proton with the adiabatic model (black line) or assuming that the proton is fixed at the terminus amine group (blue line) or at the amine group of the lysine (red line). The most stable conformations of the two latter peptides are shown in panels (b) and (c), respectively, and the direction of the dipole moment of the helix is emphasized in panel (b); the protonable amine groups are highlighted by dashed circles and ellipses.

For this peptide, the unfolding transitions look similar for all fixed protonation sites, as evidenced on the broad heat capacity peak in the 200–800 K range. As the proton is delocalized, it mainly occupies the amine end group of the first lysine, and only above 450 K does it partially transfer to the N-terminus. This value is again in good agreement with the unfolding temperature reported in other polyalanines by Kohtani et al.⁴⁴ The caloric curves reflect the average occupancies of Figure 1b. Interestingly, the most stable conformation found at low temperature with the proton on the K^* lysine also forms a $NH_2-NH_3^+$ complex and has two short strands stabilized in a beta-barrel conformation by hydrogen bond interactions between the backbone and the extended lysine side chains. In this conformation the proton is also hydrogen-bonded to the backbone. The lowest-energy structure obtained by fixing the proton on the two other sites are much more globular. Therefore, also in this case, the rather small extent of proton delocalization is due to a peculiar secondary structure.

Coupling Effects. The choice of the distance d_{NN} between the amine groups carrying the excess proton seems natural, as the bound complex formed by the NH_2 and NH_3^+ is similar to the symmetric Zundel cation between water and hydronium.⁷⁶ This feature is already captured by the adiabatic model based on Amber ff96. In Figure 5 we have represented the probability distribution of finding particular values of the distance d_{NN} , for the peptide A_4K at several temperatures simulated with the adiabatic model.

The probability is broadly distributed above the unfolding temperature, reflecting the extended random coil conformations. Near the heat capacity maximum, the distribution is bimodal

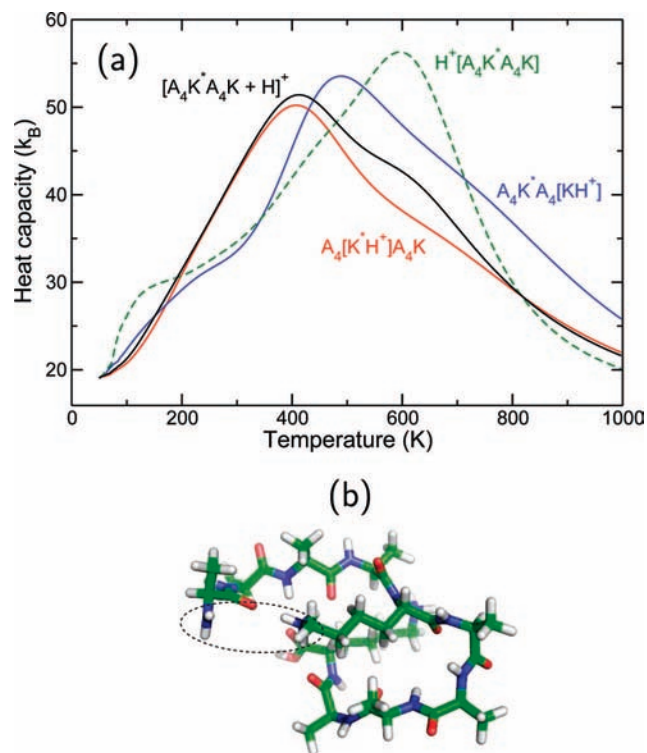


Figure 4. (a) Heat capacity of the $[A_4K^*A_4K + H]^+$ peptide obtained for the delocalized proton with the adiabatic model (black line) or assuming that the proton is fixed at the terminus amine group (dashed green line), at the amine group of the first lysine K^* (blue line), or at the amine group the second lysine K (red line). The most stable conformation, corresponding to the proton on the amine group of K^* , is shown in panel (b) with the two amine groups highlighted by a dashed ellipse.

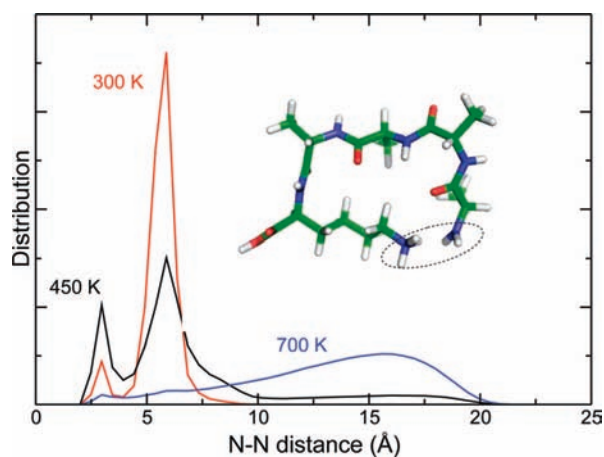


Figure 5. Probability distribution of the distance between nitrogen atoms of the two amine groups in $[A_4K + H]^+$ obtained at several temperatures, the proton being thermally delocalized in the adiabatic model. The structure corresponding to the peak at 2.6 \AA is shown as an inset, with the two amine groups highlighted in the dashed ellipse.

with two peaks centered near 2.6 and near 5.7 \AA , respectively. Conformations corresponding to the short peak have a favorable interaction between the excess proton and the NH_2 group, thus forming a proton-bound complex, as illustrated in the inset of Figure 5. Such a stable conformation is here allowed by the special geometry of the peptide, whose backbone forms two turns appropriately for the protonated lysine side chain to come into contact with the N-terminal amino group.

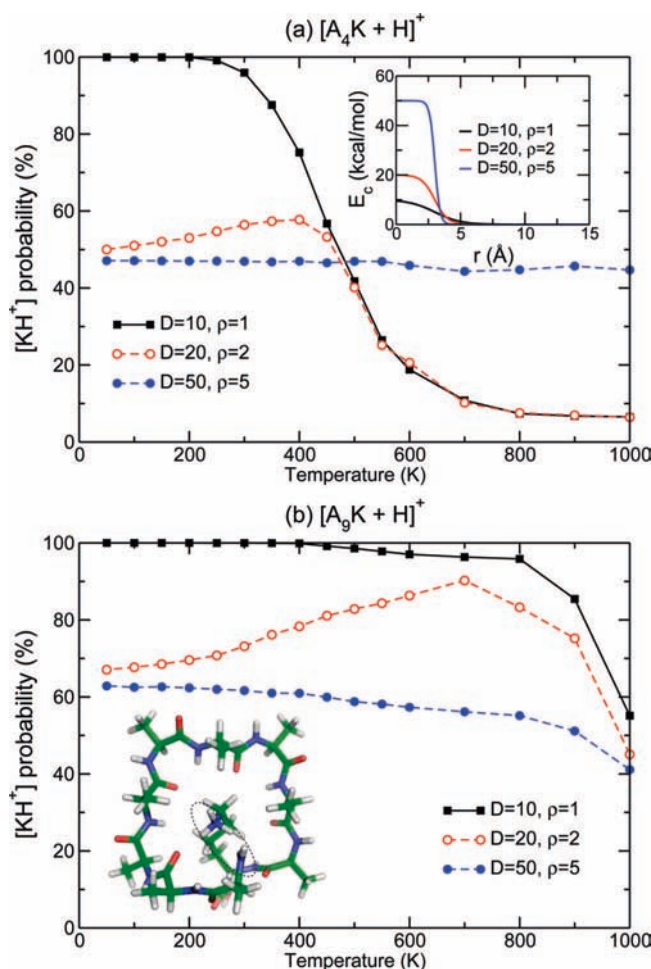


Figure 6. Occupation probability of the excess proton on the amine group of the lysine amino-acid in the $[A_4K + H]^+$ and $[A_9K + H]^+$ peptides, obtained in the coupled model with several values of the coupling constant D and the range ρ . (a) $[A_4K + H]^+$ peptide; the inset shows the variations of the coupling potential, eq 6; (b) $[A_9K + H]^+$; the inset shows the stable structure obtained at strong coupling.

When the temperature decreases further, the second peak in the distance distribution enlarges near $d_{\text{NN}} = 5.7 \text{ \AA}$, corresponding to the lowest-energy structure represented in Figure 2b. The metastability of the proton-bound conformation is, thus, the likely cause of the low-temperature shoulder in the heat capacity found in Figure 2a.

The previous investigation justifies the choice of the distance between amine groups as an order parameter for the coupling between protonable sites. We have explored the effects of such couplings by considering now the empirical valence-bond quantum Hamiltonian instead of the classical adiabatic model. The couplings, given by the diagonal elements of eq 6, are characterized by their magnitude D , their range ρ , and the cutoff d_0 . On the basis of Figure 5, we take for d_0 a value on the order of the natural d_{NN} distance in the proton-bound $[\text{NH}_2\text{-NH}_3^+]$ complex, namely, $d_0 = 3 \text{ \AA}$, allowing only D and ρ to vary.

The average occupation probabilities of the proton on the C-terminus lysine end group are shown in Figure 6 for protonated A_4K and A_9K , as a function of increasing temperature. After experimenting with the parameters, we have chosen three representative sets of binding couplings, namely $D = 10 \text{ kcal/mol}$ and $\rho = 1 \text{ \AA}^{-1}$ (weak, but long-range coupling), $D = 50 \text{ kcal/mol}$ and $\rho = 5 \text{ \AA}^{-1}$ (strong, but short-range coupling),

and $D = 20$ kcal/mol and $\rho = 2 \text{ \AA}^{-1}$ (intermediate case). The variations of the coupling energy as a function of the distance d_{NN} are sketched in the inset of Figure 6a.

In the weak coupling case, the extent of proton delocalization is very similar to the results obtained with the adiabatic approximation. Repeating the calculations with a short range does not significantly affect the results. In the opposite case of strong coupling, even at short range, the effects are generally important in the entire temperature range, and the proton is roughly half-delocalized over both sites. Monitoring the heat capacity reveals only minor variations with respect to the Dulong–Petit limit, suggesting a rigid conformation. Under such strong coupling, the proton equivalently binds to each amine group, and this binding energy is larger than the thermal energy needed to unfold the peptide. A_4K has 18 dihedral degrees of freedom, and at 1000 K the thermal energy available is thus around $18 \times k_B T \approx 36$ kcal/mol. When the intermediate coupling parameters are used, the proton is localized on the N-terminus at high temperatures, but is equally shared by the two amine receptors below the folding temperature. Examination of the structures reveals that the proton-bound conformation shown in Figure 5 is stabilized at the expense of the adiabatic global minimum.

The A_9K peptide can store a higher thermal energy before feeling the effects of the coupling. However, this molecule is also larger, and can put up with competitive proton-bound conformations. At high temperatures, the proton is shared by the two amine groups, but they do not actually form bonds. However, under strong coupling a very stable proton-bound structure is progressively stabilized as temperature decreases, as shown in the inset of Figure 6b. The resulting conformation has a square shape, the backbone making three turns and the lysine side chain making the last turn. The two amine groups lie near the middle of the square, but on each side, and interact very favorably with carbonyl oxygen atoms that are oriented toward the square center. As in the case of the smaller A_4K peptide, intermediate couplings lead to a transition to the proton-bound structure at moderate temperature, above which the proton again becomes localized on the alpha NH_2 terminus near 700 K, before getting thermally delocalized again at high temperatures. Choosing a shorter range for the weak coupling or a longer range for the strong coupling further enhance the effects (or their absence) as depicted in Figure 6.

Discussion

In the adiabatic model sampled by Monte Carlo simulations, the proton is always fixed to a specific amine group at each conformation and automatically transfers to the site with lowest potential energy. Therefore, its delocalization is statistical (thermal). The empirical valence-bond model, on the other hand, always considers the proton as partially delocalized over all available sites, for any given conformation. The extent of delocalization is quantified by the relative weights, which depend on the couplings between the states. Our present choice of attractive coupling between the amine groups favors delocalization of the proton with respect to the adiabatic case. However, upon very strong coupling the proton becomes half-delocalized over two amine groups, resulting in the apparently counter-intuitive situation where the proton can be considered as localized in the middle of these groups as the N_2H_7^+ complex.

Both models predict that delocalization should take place in all the peptides studied here, thanks to their competing basic residues (including the amine terminus), even though protonation at the amine end may be triggered only in open conformations

occurring at high temperatures. For some peptides such as A_4K , this result could be anticipated from the difference in the preferred protonation state in the fully extended and lowest-energy conformations, suggesting a transition induced by temperature. It should also be stressed here that the adiabatic model was built without any assumption about the competition between protonable sites: the relative energies are entirely described by standard force fields and dedicated first-principles calibrations. Thus, the present results provide a strong support for the mobile proton model,^{4–15} at least for the restricted case of lysine-rich polyalanines.

The main interest of our models lies in the simultaneous treatment of delocalization and temperature effects. As was shown particularly in the case of A_4K , proton delocalization can be strongly related to the folding transition. Upon an increase in temperature, transition to extended conformations can stabilize the proton onto the α amine end. This process can also be considered from the perspective of proton transfer: as the peptide is able to transfer its excess proton from the lysine end to the alpha amine, the preferred conformations change drastically, leading to unfolding. This point of view agrees with the experimental findings of Kohtani and co-workers.⁴⁴

Although temperature effects are naturally incorporated in the Monte Carlo simulations, we have not considered the possibility of transferring the proton to states that are not the lowest in energy. Such thermally activated transfers can be straightforwardly included in both the adiabatic and coupled models, by adding a discrete variable that could switch between the states, in a fashion very similar to some constant-pH algorithms.^{56,58} Preliminary simulations carried out along these lines did not indicate significant alterations with respect to the results presented here. Another possible improvement would be to treat the excess proton quantum mechanically. Beyond the numerically expensive path-integral or centroid representations, effective potentials⁷⁷ could be parametrized to include the main effects of vibrational delocalization.

A drawback of using Monte Carlo simulations is the lack of any information about the dynamics of intramolecular proton transfer. Some problems arise with the adiabatic model, where the form of eq 3 is clearly discontinuous as the proton migrates to a lower energy state. The transfer itself should then be described statistically, using stochastic molecular dynamics propagators, still not providing realistic insights into the transfer mechanisms. Using the empirical valence-bond Hamiltonian would probably be a more accurate approach for the concern of dynamics. Here, the forces should be calculated through the Hellman–Feynman theorem.^{59,60} In the short-time limit, molecular dynamics simulations performed this way could be compared with higher-level Car–Parrinello molecular dynamics. This would also open great possibilities for benchmarking the values of the coupling parameters D , ρ , and d_0 on more realistic calculations, as an alternative to the use of experimental data such as those reported in the Jarrold group.⁴⁴

Finally, other extensions of these models are worth mentioning, either for describing other basic residues such as arginine or to account for the possible protonation at amide bonds that leads to their cleavage and subsequent peptide fragmentation. Treating multiply protonated molecules would be also possible within the EVB approach, following Wang and Voth;⁷⁸ however, under high protonation states it would probably be necessary to reparametrize the force field. Modeling partially solvated peptides would also be of great interest, because intramolecular proton transfer is known to be efficiently mediated by neutral molecules such as CH_4 or N_2O ,⁷⁹ H_2 , or N_2 .^{79,80} and especially

H₂O as a catalyst.^{80–82} However, a realistic EVB approach for treating altogether one relatively large peptide surrounded by several biomolecules would require more intramolecular flexibility than was included here, especially between the donor–acceptor bonds. The EVB model developed in the Voth group,^{63,64} though suitable for molecular dynamics simulations, may remain computationally expensive in the context of large amplitude conformational changes and temperature effects.

The possibility that the proton migrates to the backbone is harder to account for within the present framework, due to the stronger perturbation exerted on the neighboring atoms. Such an extension would be probably more useful at high temperatures and for peptides lacking multiple basic residues. Again, standard density-functional theory calculations would be required to characterize all metastable states that constitute the diabatic basis set of the EVB model.

Conclusions

The amine groups of a peptide play an important role as proton carriers in the fragmentation patterns.^{9,28} In this work we have developed models for describing the possible delocalization of an excess proton over several sites of a flexible polypeptide, taking into account the large amplitude motion taking place at a finite temperature. These models rely on the empirical valence-bond formalism, through the use of force fields for the binding energy at fixed protonation state. A particular feature of these models is their assumption that the dependence of the proton affinity on the conformation can be essentially captured by the force field, up to a constant determined after calibration on some reference geometry at a higher level of theory.

The present choice of Amber ff96 was motivated here for its good performance in reproducing the properties of gas-phase peptides.⁶⁵ The effects of couplings between different protonation states were taken empirically as a monotonically decreasing function of the distance between the two amine nitrogens involved in the exchange. In absence of coupling, the adiabatic model reduces to constant-pH algorithms at fixed number of protons.^{56,58} Application of these models to the small protonated peptides A₄, A₉K, and A₄KA₄K has shown some strong interplay between temperature and proton delocalization effects on the conformation. In the adiabatic model, the proton is usually localized at low temperature on one lysine end but can partially migrate to the N-terminus. These results generally support the mobile proton model and confirm recent experimental findings by the Jarrold group⁴⁴ about the combined roles of proton transfer and temperature effects on conformational changes in peptides. They also suggest the failure of conventional force fields for such protonated peptides. Introducing attractive couplings leads to a possible stabilization of rigid proton-bound conformations.

Acknowledgment. Computer simulations were carried out at the IDRIS and CINES computer centers, which we gratefully acknowledge. We also thank GDR 2758 for financial support. We are indebted to A. R. Allouche for assistance with the DFT calculations, and we also thank D. Borgis, R. Vuilleumier, M.-P. Gaigeot, R. Antoine, M. Broyer, and I. Compagnon for fruitful discussions.

Supporting Information Available: Cartesian coordinates and Amber ff96 energies of the three peptides in their different protonation states, in their lowest-energy and extended conformations, and in proton-bound conformations. For the extended

conformations, the absolute DFT/B3LYP/6–31+G(d,p) energies are also given. This material is available free of charge via the Internet at <http://pubs.acs.org>.

References and Notes

- (1) Bountis, T., Ed. *Proton Transfer in Hydrogen-Bonded Systems; NATO ASI Series B: Physics*; Plenum Press: New York, 1992; pp 1–355. Vol 291.
- (2) Warshel, A. *Computer Modeling of Chemical Reactions in Enzymes and Solutions*; John Wiley and Sons: New York, 1991.
- (3) (a) Pinto, L. H.; Holsinger, L. J.; Lamb, R. A. *Cell* **1992**, *69*, 517–528. (b) Wang, C.; Lamb, R. A.; Pinto, L. H. *Biophys. J.* **1995**, *69*, 1363–1371. (c) Stouffer, A. L.; Nanda, V.; Lear, J. D.; DeGrado, W. F. *J. Mol. Biol.* **2005**, *347*, 169–179.
- (4) Johnson, R. S.; Martin, S. A.; Biemann, K. *Int. J. Mass. Spectrom. Ion Processes* **1988**, *86*, 137–154.
- (5) Burllet, O.; Orkiszewski, R. S.; Ballard, K. D.; Gaskell, S. J. *Rapid Commun. Mass Spectrom.* **1992**, *6*, 658–662.
- (6) McCormack, A. L.; Jones, J. L.; Wysocki, V. H. *J. Am. Soc. Mass Spectrom.* **1992**, *3*, 859–862.
- (7) Jones, J. L.; Dongré, A. R.; Somogyi, Á.; Wysocki, V. H. *J. Am. Chem. Soc.* **1994**, *116*, 8368–8369.
- (8) Papayannopoulos, I. A. *Mass Spectrom. Rev.* **1995**, *14*, 49–73.
- (9) Dongré, A. R.; Jones, J. L.; Somogyi, Á.; Wysocki, V. H. *J. Am. Chem. Soc.* **1996**, *118*, 8365–8374.
- (10) Harrison, A. G.; Csizmadia, I. G.; Tang, T.-H.; Tu, Y.-P. *J. Mass Spectrom.* **2000**, *35*, 683–688.
- (11) Schlosser, A.; Lehmann, W. D. *J. Mass Spectrom.* **2000**, *35*, 1382–1390.
- (12) Polce, M. J.; Ren, D. A.; Wesdemiotis, C. *J. Mass Spectrom.* **2000**, *35*, 1391–1398.
- (13) Wysocki, V. H.; Tsapraillis, G.; Smith, L. L.; Breci, L. A. *J. Mass Spectrom.* **2000**, *35*, 1399–1406.
- (14) El Aribi, H.; Rodriguez, C. F.; Almeida, D. R. P.; Ling, Y.; Mak, W. W.-N.; Hopkinson, A. C.; Siu, K. W. M. *J. Am. Chem. Soc.* **2003**, *125*, 9229–9236.
- (15) Paizs, B.; Suhai, S. *Mass Spectrom. Rev.* **2005**, *24*, 508–548.
- (16) (a) Pierce, W. M.; Cai, J. *Contrib. Nephrology* **2004**, *141*, 40–58. (b) Lane, C. S. *Cell. Mol. Life Sci.* **2005**, *62*, 848–869.
- (17) Biemann, K. *Methods Enzymol.* **1990**, *193*, 351–360, 455–479.
- (18) Ballard, K. D.; Gaskell, S. J. *Int. J. Mass Spectrom. Ion Process.* **1991**, *111*, 173–189.
- (19) Somogyi, Á.; Wysocki, V. H.; Mayer, I. *J. Am. Soc. Mass Spectrom.* **1994**, *5*, 704–717.
- (20) Kohtani, M.; Schneider, J. E.; Jones, T. C.; Jarrold, M. F. *J. Am. Chem. Soc.* **2004**, *126*, 16981–16987.
- (21) (a) Polfer, N. C.; Oomens, J.; Suhai, S.; Paizs, B. *J. Am. Chem. Soc.* **2005**, *127*, 17154–17155. (b) Polfer, N. C.; Oomens, J.; Suhai, S.; Paizs, B. *J. Am. Chem. Soc.* **2007**, *129*, 5887–5897.
- (22) Mueller, D. R.; Eckersley, M.; Richter, W. *J. Org. Mass Spectrom.* **1988**, *23*, 217–222.
- (23) Kenney, P. T.; Nomoto, K.; Orlando, R. *Rapid Commun. Mass Spectrom.* **1992**, *6*, 95–97.
- (24) Johnson, R. S.; Krylov, D.; Walsh, K. A. *J. Mass Spectrom.* **1995**, *30*, 386–387.
- (25) Deng, Y. Z.; Pan, H.; Smith, D. L. *J. Am. Chem. Soc.* **1999**, *121*, 1966–1967.
- (26) Demmers, J. A. A.; Rijkers, D. T. S.; Haverkamp, J.; Killian, J. A.; Heck, A. J. R. *J. Am. Chem. Soc.* **2002**, *124*, 11191–11198.
- (27) Hoerner, J. K.; Xiao, H.; Dobo, A.; Kaltashov, I. A. *J. Am. Chem. Soc.* **2004**, *126*, 7709–7717.
- (28) Jorgensen, T. J. D.; Gardsvoll, H.; Ploug, M.; Roepstorff, P. *J. Am. Chem. Soc.* **2005**, *127*, 2785–2793.
- (29) Sun, W.; Kinsel, G. R.; Marynick, D. S. *J. Phys. Chem. A* **1999**, *103*, 4113–4117.
- (30) (a) Csonka, I. P.; Paizs, B.; Lendvay, G.; Suhai, S. *Rapid Commun. Mass Spectrom.* **2000**, *14*, 417–431. (b) Paizs, B.; Suhai, S. *Rapid Commun. Mass Spectrom.* **2001**, *15*, 2307–2323.
- (31) Noguera, M.; Rodríguez-Santiago, L.; Sodupe, M.; Bertran, J. *J. Mol. Struct. (Theochem)* **2001**, *537*, 307–318.
- (32) Rodriguez, C. F.; Cunje, A.; Shoeib, T.; Chu, I. K.; Hopkinson, A. C.; Siu, K. W. M. *J. Am. Chem. Soc.* **2001**, *123*, 3006–3012.
- (33) Bleiholder, C.; Suhai, S.; Paizs, B. *J. Am. Soc. Mass Spectrom.* **2006**, *17*, 1275–1281.
- (34) Gil, A.; Simon, S.; Sodupe, M.; Bertran, J. *Theor. Chem. Acc.* **2007**, *118*, 589–595.
- (35) Li, Z.; Matus, M. H.; Velazquez, H. A.; Dixon, D. A.; Cassady, C. J. *Int. J. Mass Spectrom.* **2007**, *265*, 213–223.
- (36) Gil, A.; Bertran, J.; Sodupe, M. *J. Chem. Phys.* **2006**, *124*, 154306.
- (37) (a) Zhang, K.; Zimmerman, D. M.; Chung-Phillips, A.; Cassady, C. J. *J. Am. Chem. Soc.* **1993**, *115*, 10812–10822. (b) Klassen, J. S. A.;

- Blades, A. T.; Kebarle, P. *J. Phys. Chem.* **1995**, *99*, 15509–15517. (c) Wytenbach, T.; Bushnell, J. E.; Bowers, M. T. *J. Am. Chem. Soc.* **1998**, *120*, 5098–5103.
- (38) Hudgins, R. R.; Jarrold, M. F. *J. Am. Chem. Soc.* **1999**, *121*, 3494–3501.
- (39) Harrison, A. G. *Mass Spectrom. Rev.* **1997**, *16*, 201–217.
- (40) Bouchoux, G.; Buisson, D. A.; Colas, C.; Sablier, M. *Eur. J. Mass Spectrom.* **2004**, *10*, 977–992.
- (41) Maksič, Z. B.; Kovačević, B. *Chem. Phys. Lett.* **1999**, *307*, 497–504.
- (42) Hudgins, R. R.; Ratner, M. A.; Jarrold, M. F. *J. Am. Chem. Soc.* **1998**, *120*, 12974–12975.
- (43) Hudaky, P.; Perczel, A. *J. Phys. Chem. A* **2004**, *108*, 6195–6205.
- (44) Kohtani, M.; Jones, T. C.; Sodha, R.; Jarrold, M. F. *J. Am. Chem. Soc.* **2006**, *128*, 7193–7197.
- (45) Brooks, B. R.; Brucoleri, R. E.; Olafson, B. D.; States, D. J.; Swaminathan, S.; Karplus, M. *J. Comput. Chem.* **1983**, *4*, 187–217.
- (46) Weiner, S. J.; Kollman, P. A.; Case, D. A.; Singh, U. C.; Ghio, C.; Alagona, G.; Profeta, S.; Weiner, P. *J. Am. Chem. Soc.* **1984**, *106*, 765–784.
- (47) Van Gunsteren, W. F.; Berendsen, H. J. C. *Angew. Chem., Int. Ed. Engl.* **1990**, *29*, 992–1023.
- (48) Stillinger, F. H.; David, C. W. *J. Chem. Phys.* **1978**, *69*, 1473–1484.
- (49) (a) Halley, J. W.; Rustad, J. R.; Rahman, A. *J. Chem. Phys.* **1993**, *98*, 4110–4119. (b) Kobayashi, C.; Iwahashi, K.; Saito, S.; Ohmine, I. *J. Chem. Phys.* **1996**, *105*, 6358–6366.
- (50) Rustad, J. R. *Geochim. Cosmochim. Acta* **2005**, *69*, 4397–4410, and references therein.
- (51) Chakrabarti, N.; Roux, B.; Pomes, R. *J. Mol. Biol.* **2004**, *343*, 493–510.
- (52) Haymet, A. D.; Oxtoby, D. *J. Chem. Phys.* **1982**, *77*, 2466–2474.
- (53) Mertz, J. E.; Pettitt, B. M. *Int. J. Supercomput. Appl. High Perf. Comput.* **1994**, *8*, 47–53.
- (54) Baptista, A. M.; Martel, P. J.; Petersen, S. B. *Proteins: Struct. Funct. Genetics* **1997**, *27*, 523–544.
- (55) Börjesson, U.; Hünenberger, P. H. *J. Chem. Phys.* **2001**, *114*, 9706–9719.
- (56) Bürgi, R.; Kollman, P. A.; van Gunsteren, W. F. *Proteins: Struct. Funct. Genetics* **2002**, *47*, 469–480.
- (57) Mongan, J.; Case, D. A. *Curr. Opin. Struct. Biol.* **2005**, *15*, 157–163.
- (58) Stern, H. A. *J. Chem. Phys.* **2007**, *126*, 164112.
- (59) Vuilleumier, R.; Borgis, D. *Chem. Phys. Lett.* **1998**, *284*, 71–77.
- (60) Schmitt, U. W.; Voth, G. A. *J. Phys. Chem. B* **1998**, *102*, 5547–5551.
- (61) Cuma, M.; Schmitt, U. W.; Voth, G. A. *J. Phys. Chem. A* **2001**, *105*, 2814–2823.
- (62) Brewer, M. L.; Schmitt, U. W.; Voth, G. A. *Biophys. J.* **2001**, *80*, 1691–1702.
- (63) Maupin, C. M.; Wong, K. F.; Soudackov, A. V.; Voth, G. A. *J. Phys. Chem. A* **2006**, *110*, 631–639.
- (64) Swanson, J. M. J.; Maupin, C. M.; Chen, H. N.; Petersen, M. K.; Xu, J. C.; Voth, G. A. *J. Phys. Chem. B* **2007**, *111*, 4300–4314.
- (65) (a) Poulain, P.; Antoine, R.; Broyer, M.; Dugourd, Ph. *Chem. Phys. Lett.* **2005**, *401*, 1–6. (b) Poulain, P.; Calvo, F.; Antoine, R.; Broyer, M.; Dugourd, Ph. *Europhys. Lett.* **2007**, *79*, 66003.
- (66) Cornell, W. D.; Cieplak, P.; Bayly, C. I.; Gould, I. R.; Merz, K. M.; Ferguson, D. M.; Spellmeyer, D. C.; Fox, T.; Caldwell, J. W.; Kollman, P. A. *J. Am. Chem. Soc.* **1995**, *117*, 5179–5197.
- (67) Dinadayalane, T. C.; Sastry, G. N.; Leszczynski, J. *Int. J. Quantum Chem.* **2006**, *106*, 2920–2933.
- (68) Frisch, M. J.; Trucks, G. W.; Schlegel, H. B.; Scuseria, G. E.; Robb, M. A.; Cheeseman, J. R.; Montgomery, J. A., Jr.; Vreven, T.; Kudin, K. N.; Burant, J. C.; Millam, J. M.; Iyengar, S. S.; Tomasi, J.; Barone, V.; Mennucci, B.; Cossi, M.; Scalmani, G.; Rega, N.; Petersson, G. A.; Nakatsuji, H.; Hada, M.; Ehara, M.; Toyota, K.; Fukuda, R.; Hasegawa, J.; Ishida, M.; Nakajima, T.; Honda, Y.; Kitao, O.; Nakai, H.; Klene, Li, X.; Knox, J. E.; Hratchian, H. P.; Cross, J. B.; Bakken, V.; Adamo, C.; Jaramillo, J.; Gomperts, R.; Stratmann, R. E.; Yazyev, O.; Austin, A. J.; Cammi, R.; Pomelli, C.; Ochterski, J. W.; Ayala, P. Y.; Morokuma, K.; Voth, G. A.; Salvador, P.; Dannenberg, J. J.; Zakrzewski, V. G.; Dapprich, S.; Daniels, A. D.; Strain, M. C.; Farkas, O.; Malick, D. K.; Rabuck, A. D.; Raghavachari, K.; Foresman, J. B.; Ortiz, J. V.; Cui, Q.; Baboul, A. G.; Clifford, S.; Cioslowski, J.; Stefanov, B. B.; Liu, G.; Liashenko, A.; Piskorz, P.; Komaromi, I.; Martin, R. L.; Fox, D. J.; Keith, T.; Al-Laham, M. A.; Peng, C. Y.; Nanayakkara, A.; Challacombe, M.; Gill, P. M. W.; Johnson, B.; Chen, W.; Wong, M. W.; Gonzalez, C.; Pople, J. A. *Gaussian03*, Rev. C.02; Gaussian, Inc.: Pittsburg, PA, 2004.
- (69) (a) Mulliken, R. S. *J. Chim. Phys. Phys.-Chim. Biol.* **1964**, *61*, 20–36. (b) Warshel, A.; Weiss, R. M. *J. Am. Chem. Soc.* **1980**, *102*, 6218–6226.
- (70) Ferrenberg, A. M.; Swendsen, R. H. *Phys. Rev. Lett.* **1989**, *63*, 1195–1198.
- (71) (a) Lyubartsev, A. P.; Martynov, A. A.; Shevkunov, S. V.; Vorontsov-Velyaminov, P. N. *J. Chem. Phys.* **1992**, *96*, 1776–1783. (b) Geyer, C. J.; Thompson, E. A. *J. Am. Stat. Assoc.* **1995**, *90*, 909–920. (c) Hukushima, K.; Nemoto, K. *J. Phys. Soc. Japan* **1996**, *65*, 1604–1608.
- (72) Calvo, F. *J. Chem. Phys.* **2005**, *123*, 124106.
- (73) (a) Presta, L. G.; Rose, G. D. *Science* **1988**, *240*, 1631–1641. (b) Forood, B.; Feliciano, E. J.; Nambiar, K. P. *Proc. Natl. Acad. Sci. USA* **1987**, *84*, 8898–8902.
- (74) (a) Blagdon, D. E.; Goodman, M. *Biopolymers* **1975**, *14*, 241–245. (b) Shoemaker, K. R.; Kim, P. S.; York, E. J.; Stewart, J. M.; Baldwin, R. L. *Nature* **1987**, *326*, 563–567. (c) Richardson, J. S.; Richardson, D. C. *Science* **1988**, *240*, 1648–1652.
- (75) Wei, Y.; Nadler, W.; Hansmann, U. H. E. *J. Chem. Phys.* **2007**, *126*, 204307.
- (76) Asada, T.; Haraguchi, H.; Kitaura, K. *J. Phys. Chem. A* **2001**, *105*, 7423–7428.
- (77) Vuilleumier, R.; Borgis, D. *J. Phys. Chem. B* **1998**, *102*, 4261–4264.
- (78) Wang, F.; Voth, G. A. *J. Chem. Phys.* **2005**, *122*, 144105.
- (79) Bohme, D. K. *Int. J. Mass Spectrom. Ion Processes* **1992**, *115*, 95–110.
- (80) Chalk, A. J.; Radom, L. *J. Am. Chem. Soc.* **1999**, *121*, 1574–1581.
- (81) Gauld, J. W.; Audier, H.; Fossey, J.; Radom, L. *J. Am. Chem. Soc.* **1996**, *118*, 6299–6300.
- (82) (a) Gorb, L.; Leszczyński, J. *J. Am. Chem. Soc.* **1998**, *120*, 5024–5032. (b) Gu, J. D.; Leszczyński, J. *J. Phys. Chem. A* **1999**, *103*, 2744–2750.